ERO modelling of local deposition of injected ^{13}C tracer at the outer divertor of JET

M I Airila[1], L K Aho-Mantila[2], S Brezinsek[3], J P Coad[4], A Kirschner[3], J Likonen[1], D Matveev[3], M Rubel[5], J D Strachan[6], A Widdowson[4], S Wiesen[3] and JET EFDA Contributors‡

JET-EFDA, Culham Science Centre, OX14 3DB, Abingdon, UK

[1] VTT Technical Research Centre of Finland, Association Euratom-Tekes, P O Box 1000, 02044 VTT, Finland

[2] TKK Helsinki University of Technology, Association Euratom-Tekes, Finland

[3] Institut für Energieforschung–Plasmaphysik, Forschungszentrum Jülich, Association Euratom-FZJ, Trilateral Euregio Cluster, Germany

[4] UKAEA Fusion Association, Culham Science Centre, UK

[5] Alfvén Laboratory, Royal Institute of Technology, Association Euratom-VR, Stockholm, Sweden

[6] PPPL Princeton University, Princeton, USA

E-mail: markus.airila@vtt.fi

Abstract.

The 2004 tracer experiment of JET with injection of $^{13}CH_4$ into H-mode plasma at the outer divertor has been modelled with the Monte Carlo impurity transport code ERO. EDGE2D solutions for inter-ELM and ELM-peak phases were used as plasma backgrounds. Local 2D deposition patterns at the vertical outer divertor target plate were obtained for comparison with *post-mortem* surface analyses. ERO also provides emission profiles for comparison with radially resolved spectroscopic measurements. Modelling indicates that enhanced re-erosion of deposited carbon layers is essential in explaining the amount of local deposition. Assuming negligible effective sticking of hydrocarbons, the measured local deposition of 20–34 % is reproduced if re-erosion of deposits is enhanced by a factor of 2.5–7 compared to graphite erosion. If deposits are treated like the substrate, the modelled deposition is 55 %. Deposition measurements at the shadowed area around injectors can be well explained by assuming there negligible re-erosion but similar sticking behaviour as on plasma-wetted surfaces.

PACS numbers: 52.40.Hf, 52.65.Cc, 52.65.Pp

1. Introduction

Tracer injection experiments in tokamaks provide information on material migration and deposition under constant plasma conditions. In plasma devices with carbon plasma-

‡ See the Appendix of F Romanelli *et al* 22nd IAEA Fusion Energy Conference 2008, Geneva, Switzerland

facing components a suitable tracer is the natural isotope ^{13}C that can be distinguished from ^{12}C in *post-mortem* surface analyses. The principal carbon migration can be investigated by injecting a tracer containing molecule such as $^{13}CH_4$ from a net erosion zone, which is a strong impurity source also in the absence of injection.

Carbon migration in plasma is a complex process starting from physical or chemical erosion of the surface by particle bombardment, followed by dissociation and ionization of molecules and atoms to ions and their transport under the influence of electromagnetic forces, plasma flow and diffusion. Finally, the eroded or injected particles are deposited on the plasma-facing surfaces, where re-erosion may occur, or on remote areas. The diagnostic capabilities for studying the details of this process are limited: the density distributions of impurity species in the plasma during the discharge can be obtained *in situ* by spectroscopic measurements of their light emission (see, *e.g.* [1]), and the final tracer distribution on plasma-facing components can be measured *ex situ* by *e.g.* ion beam techniques—for an overview, see [2]. Interpretation of these measurements for complete understanding of carbon migration requires in addition computer simulations.

The modelling of global migration of ^{13}C in JET injection experiments has been completed recently and is described in a comprehensive manner in [3]. The computational tool was the 2D fluid code EDGE2D supplemented with specially tailored postprocessors to extend the modelling to re-erosion. EDGE2D uses the Monte Carlo code NIMBUS to model neutrals. The present paper reports a more detailed modelling of the local effects at the divertor which are out of reach of EDGE2D. We use the 3D impurity transport code ERO [4, 5] that has a more comprehensive physics basis for plasma–surface interaction processes, can describe the break-up chain of methane, and can cope with the toroidal inhomogeneity of the injection. Some initial modelling results that support the EDGE2D work were already reported in [3], and, conversely, the plasma solutions computed with EDGE2D are used as input for ERO in the present work.

2. Experiment

On the final experimental day of JET campaign prior to installation of the HD divertor in 2004, 31 identical discharges were run with $^{13}CH_4$ injection from 48 injection modules (GIM 10) toroidally distributed around the outer divertor. The discharges were 1.4 T, 1.4 MA H-mode with line-averaged density of 2.9×10^{19} m^{-3}, 5 MW NBI, 2.7 MW ICRH and 120 Hz 30 kJ ELMs in hydrogen plasma. During $^{13}CH_4$ puff there was no additional fuelling. The total injected amount was 4.3×10^{23} particles. The gas injection module GIM 10 is located in the gap between tiles numbered poloidally as 7 and 8. Subsequent *post-mortem* surface analysis produced deposition profiles along various measurement lines and the total amount of ^{13}C deposited on tiles 7 and 8 has been estimated to $7.3{\times}10^{22}$ particles (17 % of injection) [6]. We refer to this relative amount with the term "local deposition" or "net deposition", and in our modelling the simulation volume has been selected to match the measured area, making a direct

comparison to experiment possible. In the course of simulation the gross deposition can be several times higher than net deposition, the majority of deposit being re-eroded (see section 4.1).

Tracer injection experiments avoid the complexities characteristic for long-term plasma–wall interaction studies in which various plasma configurations are involved over a period of months or years. However, some difficulties for modelling still arise from the uncertainties in the 2004 tracer injection experiment. It was found afterwards that part of the injected methane had been able to leak behind the divertor tiles and enter the vessel on top of the outer baffle, and possibly also in the private flux region (PFR). The amount of leakage has been estimated in EDGE2D modelling [3] to be in the range 15–50 %. In modelling we have used the full injection rate, but the leakage has been taken into account when comparing modelling results to *post-mortem* analyses by scaling up the measured deposition of 17 % to 20–34 %.

Relevant diagnostics in the present experiment include surface analyses and spectroscopy. *Post-mortem* measurements of tile 7 cover the shadowed surface facing the plasma, several Rutherford backscattering spectrometry (RBS) measurements along toroidal lines, and secondary ion mass spectrometry (SIMS) measurements along two poloidal lines. The KT3 spectrometer provides 12 radially separated, line integrated signals in front of the outer divertor target. Emission lines CII at 426.7 nm, CII at 514.0 nm and CI at 909.5 nm and the CH A-X band at 431.0 nm, were acquired prior to and during the puff.

3. Simulation method

ERO is a 3D Monte Carlo impurity transport code for modelling the motion of impurity particles in plasma [*e.g.* tokamak scrape-off layer (SOL) or linear plasma simulator]. It accounts for plasma–wall interactions and relevant chemistry through external databases. The simulations proceed in discrete time steps during which the surface composition is kept constant. Within each (surface) time step a much shorter (particle) time step is used for particle tracing, which can be further decreased in the vicinity of the surface. The surface time step is limited by the requirement that one must not erode more particles than there are in the interaction layer of a surface cell. The divertor receives such a high particle flux at the strike point that (assuming a fixed 2 % chemical erosion yield and 10-fold enhanced re-erosion of deposited amorphous carbon layers) we have taken a surface time step of 0.005 seconds. The simulation volume extends 750 mm toroidally, encompassing two injector locations 560 mm apart. We have applied a periodic boundary condition for the test particles in the toroidal direction to simulate the effect of 48 injectors located around the torus. The poloidal extent is 160 mm (30 mm into the PFR and 130 mm into the SOL at target). Also the radial dimension of the volume is 160 mm.

In our modelling, we have selected as a starting point a "reference case" and carried out parameter variations in order to evaluate the significance of different assumptions

and to find out whether the match to measurements could be improved. The reference case is defined by the following input parameters: We assume the effective sticking coefficient of hydrocarbons S to be zero, describing either reflection or prompt re-erosion of deposited particles. Reflection of atoms and ions is calculated from TRIM data. The chemical erosion yield is fixed to 2 % for the substrate, but physical and chemical re-erosion of deposited material is enhanced by a factor of 10 (the effect of this number was studied with parameter variations). The temperature and flux dependence of chemical erosion have been neglected but will be later included by using the Roth formula. Particle reflection, sputtering by test particles and the background plasma, perpendicular diffusion and thermal force are included in the simulation. The total injected amount of 4.3×10^{23} molecules of $^{13}CH_4$ in the experiment was assumed to be distributed over 200 s of plasma time and evenly over the 48 injectors, giving an injection rate of 4.47×10^{19} particles/s for each source point. The plasma background is the inter-ELM EDGE2D solution with no impurities, so the only carbon sources in simulation are puffing and local erosion. Maximum ion flux to target in this plasma background is 1.4×10^{23} $m^{-2}s^{-1}$ and the flux at the puffing location 2×10^{22} $m^{-2}s^{-1}$. The external source is represented by 10 000 test particles and the eroded flux by 4800 test particles on each time step, giving good statistics for individual surface cells in most of the SOL. In the PFR (where deposition is toroidally uniform) we averaged the deposition toroidally to reduce noise. We obtained a standard deviation below 20 % except at the poloidal positions of about −25 mm and +20 mm (see figure 1). In the time traces of net deposition there are fluctuations of about 1.5 percentage units between time steps, but the fitting procedure provides the steady-state deposition with an uncertainty of about 0.2 percentage units. Tracing of the test particles in the plasma takes most of the computing time, totalling 1–3 hours per time step on a single core of a quad-core processor. About 60 iterations were needed for convergence in the reference case.

Tile 8 shadows the top edge of tile 7 from plasma so that the injected methane can possibly form a gas pocket in front of the injection location (see figure 17 of reference [3]). The dimensions of the shadowed region are a few millimetres. Significant, toroidally symmetric deposition has been found at the upper part of tile 7 [7, 8]. To model this deposition ERO would require a plasma background for particle tracing, but it is not straightforward to extend the EDGE2D plasma solution to the shadowed region and into the gap between tiles. Therefore we have simplified the tile shapes for modelling and applied a modified plasma background in ERO. Re-erosion is prevented on a surface region representing the shadow by setting the plasma temperature and density to almost zero.

4. Simulation results

4.1. Reference case

Starting from a clean carbon surface, injected ^{13}C starts building up layers mainly downstream of the injection points. At the beginning of the simulation 79 % of the injected carbon is deposited. The rest escapes into the PFR and SOL. As the layer builds up, re-erosion starts releasing some of the deposited carbon and the loss rate increases. After about 0.3 seconds of simulation time an equilibrium surface concentration distribution is reached and the net deposition rate levels off at about 17 % of the injection rate. The preferable escape route is into the PFR, some carbon still ending up into the SOL.

Figure 1 shows the deposition profiles along lines used in *post-mortem* analyses. The 2D deposition pattern for the reference case is shown in figure 2 and is relatively similar in the other cases. In these figures the modelled deposition includes 31 % excess over the steady-state deposition rate accumulated during the initial transient. One can see that the plasma flow along **B** drags the carbon downstream and that it is mostly deposited within some tens of centimetres from the source. The toroidally extending deposition stripe between injectors represents the accumulation of ^{13}C in the shadow. These two features can be seen also in the SIMS measurements. The third maximum deeper in the PFR (at -90 mm in figure 1) is not reproduced by our model.

We have compared the modelled emission patterns to the data measured during the injection, but it turned out that the measurement includes a significant contribution from the emission along the separatrix. Because we did not assume any impurities in the plasma background, our present model completely neglects this part of the emission. Therefore we cannot yet properly estimate whether ionization and dissociation are correctly described.

4.2. ELMs

As a result of the investigations of global migration [3] there are EDGE2D plasma backgrounds available both for the inter-ELM phase and for the ELM peak. The major difference between these is in temperatures. The inter-ELM plasma has $T_\mathrm{e} \approx T_\mathrm{i} < 5$ eV at the target while during ELMs target T_e reaches 130 eV and T_i exceeds 200 eV. In the present work we used these plasma solutions to perform a simple study of the effect of ELMs on local migration. Once our reference case reached its equilibrium surface composition (with the inter-ELM plasma background), successive time steps with alternating ELM-peak and inter-ELM plasma backgrounds were simulated for 145 ELM cycles (0.74 s). The lengths of the time steps were chosen to be 0.1 ms for the ELM peak and 5 ms for the inter-ELM phase, matching roughly the real durations of these phases. ELM dynamics is not completely described by this method, *e.g.* the strike point movements are neglected.

At the onset of ELMs the net deposition (over the whole cycle) drops from the

equilibrium value of 17 % to about 8 % but raises quickly (in about 0.3 s) back to about 16 %. Within individual cycles there is net erosion during ELM-peak (8–9 % of injection over the whole cycle) and net deposition between ELMs (at the beginning 17 %, then saturation at 24 %). Obviously the ELMs repeatedly deplete the deposition zone from ^{13}C, reducing its concentration in the interaction layer and thus erosion rate, which allows a higher inter-ELM net deposition rate to be sustained than in the case of a constant plasma background. Increased erosion during ELMs is due to a higher temperature and somewhat higher particle flux, which increases the physical sputtering rate to a level sufficient to cause significant erosion during the short peak-ELM phase. This way ELMs lead to some redistribution of deposited carbon, and after a short transient a new equilibrium surface distribution is obtained, however, at the SIMS measurement lines the difference between equilibria is hardly visible. Because of small ELM size (30 kJ), thermal decomposition of deposited layers should not have any significant contribution to erosion [9].

4.3. Parameter studies

Several modelling studies with the ERO code indicate that deposited soft carbon layers would be 3 to 5 times more prone to erosion than graphite [10, 11, 12]. Therefore we used a re-erosion enhancement factor f_{re}, and its value was set to 10 in our reference case. We investigated the effect of f_{re} by scanning through the range $f_{\mathrm{re}} = 1 \ldots 10$ and by interpolation we can match the measured local deposition with $f_{\mathrm{re}} = 2.5 \ldots 7$. This is illustrated in figure 3 (red bars) where the experimental range accounts for the uncertainty due to methane leakage. Deposition on plasma-wetted surfaces depends inversely on f_{re}, while the deposition in shadow is essentially independent on f_{re}, resulting in the nonlinear dependence shown. Local deposition in other simulation cases is also included in the figure (blue bars, see below). The assumption of enhanced re-erosion is also supported by the comparison to SIMS (figure 1): without it the poloidal deposition maximum is much wider and does not show the double-peak structure visible in measurements between the outer strike point (OSP) and puffing location. Such a profile from initial simulations of the present work is shown in figure 10 of reference [3] and illustrates that ERO and EDGE2D give very comparable results if the shadow model and enhanced re-erosion are suppressed.

In the EDGE2D/NIMBUS work [3] it was assumed that the injected $^{13}CH_4$ can be described as ^{13}C atoms. To estimate the validity of this assumption we have run ERO also by injecting atoms instead of molecules. To make the comparison meaningful, the injection energies and sticking behaviour of atoms/molecules must be similar in both cases. ERO uses by default a thermal distribution of molecules whereas in fluid codes the emission energy of atoms is typically of the order of break-up energy of CH_4 (about 0.5 eV) [13]. The energy dependence was investigated by simulating atomic injection with 0.05 eV and 1 eV. Moreover, in ERO the reflection of atoms and ions is calculated from TRIM data. To separate also this effect, we needed an additional simulation case

with molecular injection and $S = 0.7$ for hydrocarbons (corresponding to the typical reflection coefficient of 0.3 from TRIM). In this high-sticking case the deposition pattern becomes much more peaked than the measured one and local deposition is too high (bar 5 in figure 3). With atomic injection at 0.05 eV the result is similar (bar 6). With a higher injection energy (bar 7) the local deposition drops by some 50 %, which compensates for the higher sticking, and the locally deposited fraction in fact coincides with measurements. Estimating the local source provided by the present results for global migration modelling requires a more detailed evaluation of particle losses and will be given in another contribution [8]. As an additional parameter variation we will also combine the cases $S = 0.7$ and "no shadow" – two counteracting mechanisms with respect to the reference case.

If the shadow model is disabled, the deposition pattern peaks strongly in the vicinity of injectors. Therefore the high measured deposition in the shadow along "SIMS A" measurement line cannot reproduced. Also the amount locally deposited (about 7 %) remains much below the measured value.

Finally, the calculation of test particle motion in ERO is based on a relaxation time approximation of the Fokker-Planck equation and requires that one explicitly specifies the distribution functions for all plasma particle species. In the derivation it is assumed that these distributions are Maxwellian. Due to parallel temperature gradients in the plasma, higher-order corrections, thermal forces, are needed for a more accurate description. We have implemented the calculation of thermal forces for the divertor version of ERO. The temperature gradients are evaluated from the EDGE2D plasma solution by a preprocessor. In the present simulation cases the gradients are of the order 6×10^{-2} eV/mm in the poloidal plane, but $\mathbf{B}$ is nearly toroidal. Therefore the gradients projected along $\mathbf{B}$ are as weak as 4×10^{-3} eV/mm and the effect of thermal force remains negligible.

5. Summary

Local deposition in the 2004 JET divertor tracer injection experiment was carried out with the ERO code using EDGE2D plasma backgrounds. Measured ^{13}C distributions can be closely reproduced by assuming negligible effective sticking of hydrocarbons, enhanced re-erosion of deposits and no re-erosion in the shadowed areas. Sensitivity of the results was studied with parameter variations and the effect of ELMs addressed by using different fluid plasma solutions in ERO. The spectroscopy analysis will be improved, which helps validating the ionisation/dissociation data used in ERO. The present results also raise needs for additional parameter variations. *E.g.* the inclusion of neutrals, in particular charge-exchange atoms, may have a significant effect locally due to dissociation of the injected methane. Modelling of gap deposition will be carried out by interfacing ERO with the 3DGap code [14] for more realistic geometry description.

Acknowledgments

We have used computing services provided by CSC – IT Center for Science Ltd.

References

[1] Brezinsek S *et al* 2007 *J. Nucl. Mat.* **363–365** 1119
[2] Rubel M *et al* 2005 *Vacuum* **78** 255
[3] Strachan J D *et al* 2008 *Nucl. Fusion* **48** 105002
[4] Naujoks D *et al* 1993 *Nucl. Fusion* **33** 581
[5] Kirschner A *et al* 2000 *Nucl. Fusion* **40** 989
[6] Coad J P *et al* 2007 *J. Nucl. Mat.* **363–365** 287
[7] Coad J P 2008 Local deposition of the ^{13}C tracer at the JET MkII-SRP outer divertor *9th Int. Workshop on Hydrogen Isotopes in Fusion Reactor Materials (Salamanca)*
[8] Airila M I *et al* 2009, to be submitted
[9] Kreter A *et al* 2009 *Phys. Rev. Lett.* **102** 045007
[10] Wienhold P *et al* 2001 *J. Nucl. Mat.* **290–293** 362
[11] Kirschner A *et al* 2004 *J. Nucl. Mat.* **328** 62
[12] Kirschner A etal 2003 *Plasma Phys Control. Fusion* **45** 309
[13] Stamp M *et al* 1999 *J. Nucl. Mat.* **266–269** 685
[14] Matveev D 2008 *Modelling of material deposition in the gaps of castellated surfaces in fusion experiments* Master thesis (Ghent University)

Figure captions

Figure 1. Poloidal profiles of the deposition along SIMS measurement lines in the reference case. Lines: ERO simulation, markers: SIMS measurements along the lines shown in figure 2. Left from the OSP the profile has been toroidally averaged to reduce noise.

Figure 2. Top: Illustration of one toroidal period of the outer divertor. Bottom: Deposition pattern in the reference simulation. Injector locations are marked with "x", the shadow extends toroidally across them and SIMS measurement lines are shown in grey.

Figure 3. Local deposition with different values of the re-erosion enhancement factor f_{re} (red bars) and for various cases with other modelling assumptions (blue bars). Case 1: Reference case (shadow and thermal force included, molecular injection, $S = 0$, $f_{\mathrm{re}} = 10$). Match to experiment is achieved with $f_{\mathrm{re}} = 2.5 \ldots 7$. Cases 2 to 4: As reference but $f_{\mathrm{re}} = 5, 2, 1$, respectively. Case 5: As reference but $S = 0.7$. Cases 6 and 7: As reference but atomic injection at 0.05 eV and 1 eV, respectively. Case 8: As reference but without shadow. Case 9: As reference but without thermal force.

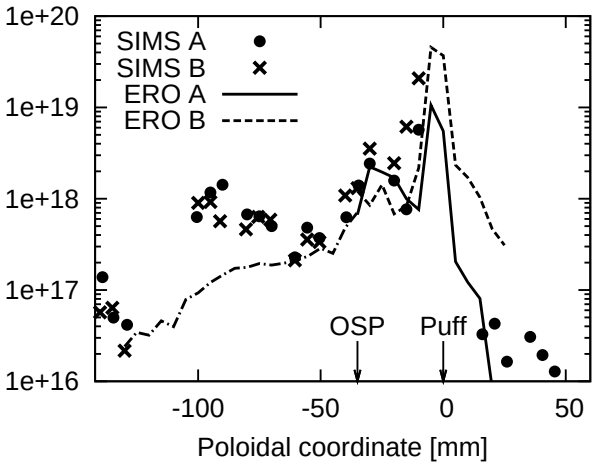
1e+20
1e+19
1e+18
1e+17
1e+16
SIMS A
SIMS B
ERO A
ERO B
OSP
Puff
-100
-50
0
50
Poloidal coordinate [mm]

Figure 1

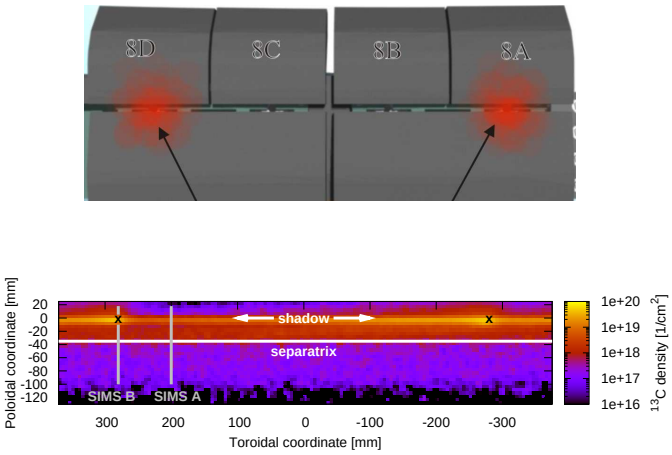
8D
8C
8B
8A
Poloidal coordinate [mm]
20
0
-20
-40
-60
-80
-100
-120
shadow
separatrix
SIMS B
SIMS A
300
200
100
0
-100
-200
-300
Toroidal coordinate [mm]
1e+20
1e+19
1e+18
1e+17
1e+16
^{13}C density [1/cm^2]

Figure 2

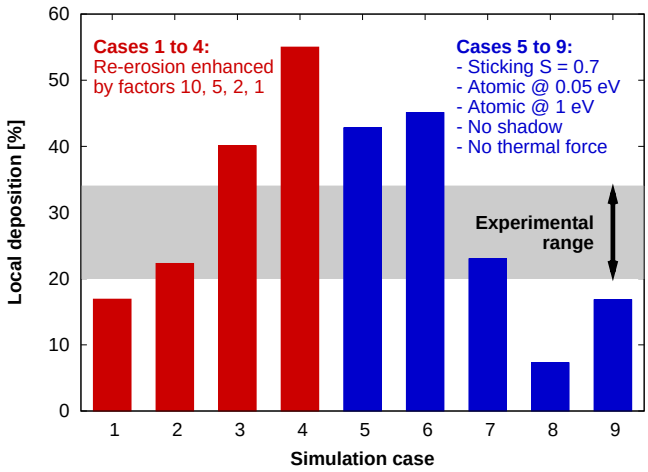
Cases 1 to 4:
Re-erosion enhanced
by factors 10, 5, 2, 1
Cases 5 to 9:
- Sticking S = 0.7
- Atomic @ 0.05 eV
- Atomic @ 1 eV
- No shadow
- No thermal force
Experimental
range
Local deposition [%]
Simulation case
0
10
20
30
40
50
60
1
2
3
4
5
6
7
8
9

Figure 3